



Application Performance Modeling via Tensor Completion

Edward Hutter

hutter2@illinois.edu

Department of Computer Science

University of Illinois at Urbana-Champaign

Champaign, IL, USA

Edgar Solomonik

solomon2@illinois.edu

Department of Computer Science

University of Illinois at Urbana-Champaign

Champaign, IL, USA

ABSTRACT

Performance tuning, software/hardware co-design, and job scheduling are among the many tasks that rely on models to predict application performance. We propose and evaluate low-rank tensor decomposition for modeling application performance. We discretize the input and configuration domains of an application using regular grids. Application execution times mapped within grid-cells are averaged and represented by tensor elements. We show that low-rank canonical-polyadic (CP) tensor decomposition is effective in approximating these tensors. We further show that this decomposition enables accurate extrapolation of unobserved regions of an application’s parameter space. We then employ tensor completion to optimize a CP decomposition given a sparse set of observed execution times. We consider alternative piecewise/grid-based models and supervised learning models for six applications and demonstrate that CP decomposition optimized using tensor completion offers higher prediction accuracy and memory-efficiency for high-dimensional performance modeling.

ACM Reference Format:

Edward Hutter and Edgar Solomonik. 2023. Application Performance Modeling via Tensor Completion. In *The International Conference for High Performance Computing, Networking, Storage and Analysis (SC ’23), November 12–17, 2023, Denver, CO, USA*. ACM, New York, NY, USA, 13 pages. <https://doi.org/10.1145/3581784.3607069>

1 INTRODUCTION

Application performance depends on both configuration parameters (e.g., block sizes, processor grid topology) and architectural parameters (e.g., processes-per-node, hyper-thread count) for a given set of inputs. Complex interactions among these parameters [54, 68] motivate observation of an application’s full parameter space, the size of which has increased to account for growth in algorithmic complexity and architectural diversity. Tasks such as program optimization [5, 18, 49], optimal tuning parameter selection [36, 54], architectural design [31, 32], dynamic load balancing, and machine allocation estimation (e.g., for weather forecasting) increasingly rely upon predictive models for accurate and efficient performance prediction.

Permission to make digital or hard copies of all or part of this work for personal or classroom use is granted without fee provided that copies are not made or distributed for profit or commercial advantage and that copies bear this notice and the full citation on the first page. Copyrights for components of this work owned by others than the author(s) must be honored. Abstracting with credit is permitted. To copy otherwise, or republish, to post on servers or to redistribute to lists, requires prior specific permission and/or a fee. Request permissions from permissions@acm.org.

SC ’23, November 12–17, 2023, Denver, CO, USA

© 2023 Copyright held by the owner/author(s). Publication rights licensed to ACM.

ACM ISBN 979-8-4007-0109-2/23/11...\$15.00

<https://doi.org/10.1145/3581784.3607069>

The demand for increasingly accurate performance prediction is reflected in the abundance of available performance modeling frameworks (e.g., [4, 7, 8, 64]). Application performance models, which we survey in Section 3, are typically either (1) global (non-piecewise) models configured semi-analytically or automatically (such as via *performance model normal form* [4, 5]), (2) piecewise/grid-based models, which discretize the modeling domain (such as *sparse grid regression* (SGR) [50]), or (3) alternative models configured by supervised learning methods (such as neural networks). We instead consider tensor decompositions, which generalize low-rank matrix factorizations to higher dimensions [29] and are effective models for tensor completion [1, 67], the problem of approximating a tensor given a subset of observed entries. Specifically, we employ tensor completion based on low-rank CP decomposition [17] for application performance modeling, and compare this model, which belongs to type (2), to representative models of each type.

A CP decomposition models an application configuration $\mathbf{x} \equiv (x_1, \dots, x_d)$ ’s execution time $f(\mathbf{x})$ as a linear combination of separable piecewise functions $m(\mathbf{x}) = \sum_{r=1}^R \prod_{j=1}^d g_{r,j}(x_j)$. A CP decomposition thus generalizes simple multilinear execution cost models. These models also provide systematic improvability (via increased rank) and achieve linear model size with tensor order (number of application parameters) for a fixed rank. We provide specific details on how we discretize an application’s parameter space to construct a low-rank CP decomposition model in Section 5.

We evaluate this model in two settings: interpolation (training set sampled from same input and configuration domain as test set) and extrapolation (test set contains larger scale problems than training set). We consider an error metric $|\log(m(\mathbf{x})/f(\mathbf{x}))|$ that is independent of the scale of the execution times. To minimize this error, we consider two loss functions. First, we simply transform the input data and minimize $(\hat{m}(\mathbf{x}) - \log(f(\mathbf{x})))^2$, resulting in model $m(\mathbf{x}) = e^{\hat{m}(\mathbf{x})}$. Second, we consider loss function $\log(m(\mathbf{x})/f(\mathbf{x}))^2$, which requires enforcing positivity of an alternative model $m(\mathbf{x})$. The positivity of the latter model is leveraged by our proposed method for extrapolation, as it employs rank-1 factorizations that retain positivity.

The most similar technique to CP decomposition studied in prior work for application performance modeling is *sparse grid regression* (SGR) [46, 50]. SGR uses a hierarchical reduced-size model of a regular grid containing performance measurements, whereas we first discretize an application’s parameter space directly on a regular grid before formulating a CP decomposition of the corresponding tensor. Both SGR and CP decomposition can compress performance across high-dimensional modeling domains efficiently. Our experimental results in Section 7 show that low-rank CP decomposition offers improved accuracy and scalability in high-dimensional domains, and further facilitates accurate performance extrapolation.

Our experimental evaluation considers randomly sampled execution times of 6 benchmarks: QR factorization, matrix multiplication, MPI Broadcast, ExaFMM [72], AMG [53], and KRIPKE [30] on the Stampede2 supercomputer [61]. These applications have 2-12 parameters (including input parameters, configuration parameters, and architectural parameters), yielding tensors of corresponding order in our model. Our experiments consider 9 alternative methods: sparse grid regression, multi-layer perceptrons, random forests, gradient-boosting, extremely-randomized trees, Gaussian process regression, support vector machines, adaptive spline regression, and k-nearest neighbors. Among these methods, we find our tensor model to be the most effective in multiple metrics, including model accuracy and model size. Our model is especially efficient in comparison to other models for applications with high-dimensional (many parameter) input and configuration domains.

Our novel contributions towards application performance modeling are as follows:

- a methodology for learning piecewise multilinear models via application of CP tensor decomposition (CPR),
- a technique for performance extrapolation using CP tensor decomposition,
- a software library for CPR that leverages open-source high-performance software for tensor completion¹,
- an evaluation of piecewise/grid-based models and alternative supervised learning methods using six applications,
- empirical evidence that CPR achieves highest prediction accuracy among existing models relative to model size.

2 PROBLEM STATEMENT

Application performance models predict execution times given a configuration of application benchmark parameters. We formalize performance modeling and summarize quantitative techniques to assess performance models in this section.

2.1 Modeling Problem

We consider the problem of predicting execution times of an application for any configuration (i.e., selection of parameter values for each of a pre-specified set of parameters), given execution times of an observed subset of an application’s parameter space. Formally, the execution time of an application is represented by a latent multivariate function $f : \mathcal{X} \rightarrow \mathbb{R}^+$, which attributes positive real values to all configurations across its d -dimensional parameter space $X^{(1)} \times \dots \times X^{(d)} \equiv \mathcal{X}$. Each configuration $(x_1, \dots, x_d) \equiv \mathbf{x} \in \mathcal{X}$ is comprised of input parameters (e.g., matrix dimension), configuration parameters (e.g., block size), and/or architectural parameters (e.g., thread count). These parameters may be real, of integer type, or categorical (e.g., choice of solver). In the absence of a set of benchmark parameters, statistical techniques (e.g., clustering and correlation analysis [31, 32]), which we do not evaluate, can facilitate specification of configuration space \mathcal{X} .

A performance model $m : \tilde{\mathcal{X}} \rightarrow \mathbb{R}$ maps a d -parameter configuration $\mathbf{x} \in \tilde{\mathcal{X}}$ to a real value $m(\mathbf{x})$, which represents a prediction of true execution time $f(\mathbf{x})$. The modeling domain $\tilde{\mathcal{X}} \subseteq X^{(1)} \times \dots \times X^{(d)}$ is a subset of an application’s configuration space

¹<https://github.com/huttered40/cpr-perf-model>

Metric	Mathematical Expression	Error Expression
MAPE	$\sum_{k=1}^M \frac{ m_k - y_k }{y_k}$	$\sum_{k=1}^M \epsilon_k $
MAE	$\sum_{k=1}^M m_k - y_k $	$\sum_{k=1}^M y_k \epsilon_k $
MSE	$\sum_{k=1}^M (m_k - y_k)^2$	$\sum_{k=1}^M (y_k \epsilon_k)^2$
SMAPE	$2 \sum_{k=1}^M \frac{ m_k - y_k }{y_k + m_k}$	$2 \sum_{k=1}^M \left \frac{\epsilon_k}{2 + \epsilon_k} \right $
LGMAPE	$\sum_{k=1}^M \log\left(\frac{ m_k - y_k }{y_k}\right)$	$\sum_{k=1}^M \log(\epsilon_k)$
MLogQ	$\sum_{k=1}^M \log\left(\frac{m_k}{y_k}\right) $	$\sum_{k=1}^M \left \frac{\epsilon_k}{1 + \epsilon_k} \right + O(\epsilon_k^2)$
MLogQ2	$\sum_{k=1}^M \log^2\left(\frac{m_k}{y_k}\right)$	$\sum_{k=1}^M \left(\frac{\epsilon_k}{1 + \epsilon_k} \right)^2 + O(\epsilon_k^4)$

Table 1: Error metrics and corresponding expressions (scaled by M) given model predictions m , true positive outputs y , and errors $\epsilon = m/y - 1$. Both expressions are equivalent across rows 1-5, and equivalent to low-order Taylor approximation in ϵ across rows 6-7.

\mathcal{X} , and is ascertained either from a set of previously executed configurations (i.e., training set) or by intuition. Configurations outside of the modeling domain $\mathbf{x} \notin \tilde{\mathcal{X}}$ induce extrapolation, while configurations within the modeling domain $\mathbf{x} \in \tilde{\mathcal{X}}$ induce interpolation. The prediction accuracy of a performance model should be robust to extrapolation and generalize effectively for interpolation. We evaluate both settings for model inference in Section 7.

Predictive models for estimating application performance can be classified as analytic, learned (i.e., data-driven), or some combination therein. Analytic models rely on program analysis and/or expert knowledge of both an application and architecture, and decompose an application’s execution time into execution times contributed by computational and communication kernels executed along its execution call paths [12, 15, 18, 19, 28, 52, 64]. Domain expertise and static source code analysis alone have been shown to achieve sufficient accuracy in modeling performance to facilitate optimal configuration selection for both non-distributed kernels [33, 34, 37] and distributed kernels [14, 47]. We instead consider and evaluate learned models for estimating application performance that are configured solely using execution times of observed configurations.

2.2 Model Assessment

Performance models may be assessed in terms of model size, optimization complexity, inference time, and/or the accuracy with which they predict application performance. Given a particular configuration of application parameters $(x_1, \dots, x_d) \equiv \mathbf{x}$, execution time $y \equiv f(\mathbf{x})$ acquired by averaging a sufficient number of samples, and a model output $m \equiv m(\mathbf{x})$, relative prediction error is given by $|m - y|/y$. While relative error is more appropriate than absolute error for assessing performance predictions spanning multiple orders of magnitude (e.g., application evaluation over a range of inputs), it does not assign similar errors to mispredictions of a similar scale (i.e., $|\log(m/y)|$). Model selection via minimization of relative error exhibits bias towards under-prediction [66], which can misinform tasks that leverage model output (e.g., optimal parameter selection).

To assess performance prediction accuracy, we adopt error metrics that assign equal error to under/over-predictions of the same scale (i.e., scale independence). In particular, we penalize model outputs $m_k = ay_k$ and $\tilde{m}_k = y_k/a$ equally for positive factor a . Consider a collection of measured configurations $\{(\mathbf{x}_k, y_k)\}_{k=1}^M$ and model

outputs $\{(\mathbf{x}_k, m_k)\}_{k=1}^M$. Among the aggregate error metrics listed in Table 1, only the arithmetic means of the absolute log and log-squared accuracy ratios (MLogQ and MLogQ2, respectively) achieve scale independence [45, 66]. This table also demonstrates the equivalence of the symmetric mean and log-transformed geometric-mean relative errors (SMAPE and LGMAPE, respectively), and MLogQ to first-order Taylor approximation for small relative errors ϵ_k defined as $m_k = y_k(1 + \epsilon_k)$. We configure models to minimize MLogQ in Section 6, and describe alternative loss functions that target this in Sections 5.2 and 5.3.

3 MULTI-PARAMETER PERFORMANCE MODELING

Application performance modeling uses model class selection and optimization to minimize an application-dependent error metric. Selection of a class of models reflects application characteristics (e.g., scaling behavior, discontinuities) identified analytically and/or learned using measurements of executed configurations. Following a selection of class-specific hyper-parameters, a candidate model is configured by minimizing an aggregate error metric on execution times of observed configurations. We review methods to construct performance models that address the modeling problem described in Section 2.1.

3.1 Global

Relationships between application benchmark parameters and execution times are expressed as linear combinations of predictor variables (i.e., non-piecewise functions parameterized on a subset of benchmark parameters), each of which has global support across the parameter space. These variables model interaction effects and nonlinear scaling behavior among subsets of parameters. Ordinary least-squares regression (OLS) is a quadratic optimization problem that estimates unknown parameters expressed linearly with respect to predictor variables by minimizing mean squared error (MSE). Use of OLS or ridge regression to optimize global models were among the first class of methods proposed for modeling application performance empirically [3, 15, 31, 32] and remain widely used, especially in settings in which a limited number of configurations can be executed.

Expert insight, statistical analysis, and automated search have each been proposed to find suitable predictor variables to instantiate interpretable global models with varying complexity. Adaptations to Lasso regression have been shown to effectively prune a large space of predictors [21]. Alternative methods to circumvent statistical analyses for predictor selection include symbolic regression [6] and search, which performs OLS repeatedly on candidates from canonical classes of small global models. In particular, the performance model normal form [4, 5] expresses execution time as

$$m(\mathbf{x}) = \sum_{r=1}^R \alpha_r \prod_{j=1}^d x_j^{v_{r,j}} \log^{w_{r,j}}(x_j), \quad (1)$$

which defines a search space, the size of which is predicated on user-specified sets of rational numbers v, w . Global models that utilize log-transformed benchmark parameters as predictors significantly reduce this predictor search space while retaining tolerable prediction accuracy [3].

3.2 Piecewise/Grid

Non-piecewise predictor variables can be insufficient for modeling complex performance behavior with high accuracy. Complex dependence of performance on application parameters arises even in simple programs due to e.g., memory misalignment, register spilling, and load imbalance. This behavior can be more accurately modeled as a linear combination of spline functions, i.e., tensor products of univariate functions defined piecewise by polynomials. These models introduce additional hyper-parameters, notably the selection of grid-points that discretize the modeling domain. Therefore, it is common to formulate global models, and only segment those parameters whose values correlate strongest with performance [31, 32].

Multilinear interpolation methods evaluate an application's execution time $f(\mathbf{x})$ on d -dimensional regular grids and model $f(\mathbf{x})$ as a weighted average of 2^d neighboring grid-points, each of which stores the measured execution time of a distinct configuration. For example, bilinear interpolation predicts a configuration (x_1, x_2) 's execution time as

$$m(\mathbf{x}) = \sum_{a=i_1}^{i_1+1} \sum_{b=i_2}^{i_2+1} t_{a,b} \left(1 - \frac{|x_1 - x_a|}{x_{i_1+1} - x_{i_1}} \right) \left(1 - \frac{|x_2 - x_b|}{x_{i_2+1} - x_{i_2}} \right),$$

where $x_{i_j} \leq x_j < x_{i_j+1}, \forall j \in \{1, 2\}$ and $t_{a,b}$ denotes the execution time of grid-point (a, b) on a two-dimensional regular grid. Multilinear interpolation is suitable if performance behavior within grid-cells is sufficiently smooth. However, this is rarely achieved without a significantly large number of observations.

Multiple frameworks, including *multivariate adaptive regression splines* (MARS)[11] and *sparse grid regression* [50, 51], instead compress regular grids by selecting a subset of grid-points and corresponding spline functions automatically. MARS recursively constructs products of univariate hinge functions $h(x_i) = \{c, \max(0, x_i - c)\}$, each characterized by a parameter x_i and a scalar position c within its range. The selection of these parameters involves repeatedly searching across the parameter space and invoking OLS as candidate models are constructed and pruned. We observe in Section 7 that MARS performance models [9] achieve only a coarse discretization of high-dimensional modeling domains and often produce global models.

Sparse grid regression (SGR) discretizes high-dimensional functions on anisotropic sparse grids. Sparse grids [13, 58, 73] are characterized by a hierarchical representation of piecewise-linear functions, the tensor-product of which yields piecewise d -linear basis functions. Only functions with sufficiently-large support across the modeling domain are retained. Sparse grids initially utilize $O(2^n n^{d-1})$ grid-points, where n is a user-specified discretization level. SGR models an application's execution time as a linear combination of $O(2^n n^{d-1})$ multi-scale basis functions [46] and offers automated spatially-adaptive grid refinement within the support of a specified number of basis functions [46]. Our methodology circumvents grid refinement and compresses regular grids, which feature $O(2^{nd})$ total grid-points, using rank- R tensor decompositions to $O(2^n dR)$ size. We evaluate both methods in Section 7.

3.3 Neural Networks

Neural networks express execution time as a nonlinear composition of weighted summations, and thereby circumvent predictor selection and modeling domain discretization. Feed-forward multi-layer perceptrons (MLP) were among the first neural network architectures evaluated for performance modeling [23, 32]. The architectures of these models consist of stacks of layers, each containing an array of units characterized by weights and an activation function. Subsequent studies have compared the prediction accuracy of MLPs against other black-box methods [40] and explored their use as a cost model to guide optimal parameter selection [65]. Optimization of MLPs using training data at distinct process counts has been shown to facilitate incremental extrapolation for large-scale scientific simulations [41]. MLPs have additionally been used to generate embeddings (i.e., fixed-size vectors) for variable-length features (e.g., instructions within loop nests) extracted from source code as inputs to more sophisticated architectures. Some of these architectures include recurrent and/or recursive neural networks, which have been evaluated to predict throughput of a block of instructions [43, 63], deep-learning pipelines [62], and to facilitate automatic code generation [2]. Additionally, graph neural networks can be formulated from directed acyclic graph representations of compiled source code to predict throughput of tensor-based workloads [27]. As these models rely on significantly large and un-parameterized training sets, we do not evaluate them. We instead evaluate MLP architectures, which themselves feature a large design space, on parameterized training sets.

3.4 Kernel-based

Kernel methods project the modeling domain onto a higher-dimensional space characterized by user-specified kernel functions (e.g., sigmoid). Support vector machines (SVM) are global models formulated by partitioning the modeling domain so as to minimize a weighted distance between model predictions and observed performance. Gaussian process (GP) regression assumes that observations are samples of a multivariate normal distribution, and are characterized by a mean vector and a positive-definite covariance matrix. Although both methods have been evaluated for performance modeling [40], they are best-suited when limited training data is available and/or when it is acquired incrementally (e.g., to guide optimal parameter selection [10, 44, 68]). Recent works advance and generalize the use of GPs for learning application performance across independent problems (i.e., multi-task learning) by proposing use of linear combinations of GPs [36], piecewise-additive GPs [38], and deep GPs [39]. We evaluate both SVMs and basic GP regression models in this work.

3.5 Recursive Partitioning

Decision trees partition the modeling domain into hyper-rectangles, each of which is assigned a constant value that models the execution time of configurations mapped within its sub-domain. These hyper-rectangles are constructed by recursively splitting a parameter's range to minimize a loss function (e.g., MSE) on a subset of observations. Random forest regression models execution time as an average of these constants; each tree is constructed using a random sample of observations via bootstrap aggregation, while

each tree's splits are constructed by minimizing a loss on a random sample of a subset of observations. Extremely-randomized tree regression, which has been shown to be among the most accurate methods for performance modeling [22, 24, 40, 41], computes splits randomly instead of minimizing a specified error metric. Gradient-boosting regression constructs trees sequentially by fitting residuals attained by the previously-constructed sequence of trees, which are proportional to the negative gradients of the chosen loss function. These methods have each been evaluated to construct surrogate models within a Bayesian optimization framework to guide optimal parameter selection [70, 71]. In our experimental evaluation, we tune over a subset of hyper-parameters shared by each method, including forest size (i.e., number of trees) and tree-depth.

3.6 Instance-based

Instance-based methods construct models on-the-fly using execution times of observed configurations. We evaluate the k -nearest neighbors method, which predicts execution time by interpolating the execution times of the k nearest observed configurations relative to a specified distance metric, and which has been previously evaluated for modeling application performance [40].

4 TENSOR COMPLETION

Tensor completion is the task of building a model to approximate a tensor based on a subset of observed entries [1, 35]. A low-rank tensor factorization is typically used to model a partially-observed tensor, which is optimized via tensor completion. We review models and optimization methods for tensor completion in this section.

4.1 Low-Rank Tensor Factorization

A tensor $\mathcal{T} \in \mathcal{R}^{I_1 \times \dots \times I_d}$ has order d (i.e., d modes/indices), dimensions I_1 -by- \dots -by- I_d , and elements $t_{i_1, \dots, i_d} \equiv t_i$ where $i \in \otimes_{j=1}^d \{1, \dots, I_j\}$. A tensor exhibiting low-rank structure can be approximated as a summation of tensor products (i.e., canonical-polyadic decomposition [17]) or using other tensor factorizations such as Tucker [29]. The canonical-polyadic (CP) decomposition of an order three tensor $\mathcal{T} \in \mathcal{R}^{I_1 \times I_2 \times I_3}$ has the form

$$t_{i_1, i_2, i_3} \approx \sum_{r=1}^R u_{i_1, r} v_{i_2, r} w_{i_3, r} \equiv \hat{t}_{i_1, i_2, i_3}, \quad (2)$$

where R denotes the rank of the decomposition, and $\mathbf{U} \in \mathcal{R}^{I_1 \times R}$, $\mathbf{V} \in \mathcal{R}^{I_2 \times R}$, $\mathbf{W} \in \mathcal{R}^{I_3 \times R}$ are factor matrices. The size of a CP decomposition grows linearly with tensor order for fixed dimensions and fixed CP rank, and linearly with CP rank for a fixed order and fixed dimensions. Tensor completion is an effective technique to attain a low-rank CP decomposition when only a subset of tensor elements are observed [1, 67].

A CP decomposition optimized via tensor completion should accurately represent observed tensor entries, yet generalize effectively to unobserved entries. The set of observed entries of an order-3 tensor \mathcal{T} is represented by an index set $\Omega \subseteq \{1, \dots, I_1\} \times \{1, \dots, I_2\} \times \{1, \dots, I_3\}$ so that every element $i \equiv (i_1, i_2, i_3) \in \Omega$ has an associated observation $t_i \equiv t_{i_1, i_2, i_3}$. Tensor completion involves minimizing an objective function that consists of a convex loss function and regularization terms in each factor matrix. Regularization decreases model parameter variance and thereby avoids

over-fitting to observed entries. The choice of element-wise loss function ϕ reflects both the distribution of observed elements and the selected error metric. Given an observed dataset Ω , CP rank R , and regularization parameter λ , methods for tensor completion with CP decomposition of an order-3 tensor minimize the objective function $g(U, V, W) =$

$$\lambda(\|U\|_F^2 + \|V\|_F^2 + \|W\|_F^2) + \sum_{(i_1, i_2, i_3) \in \Omega} \phi(t_{i_1, i_2, i_3}, \hat{t}_{i_1, i_2, i_3}). \quad (3)$$

Minimization of Equation 3 using least-squares loss functions $\phi(t_{i_1, i_2, i_3}, \hat{t}_{i_1, i_2, i_3}) = (t_{i_1, i_2, i_3} - \hat{t}_{i_1, i_2, i_3})^2$ and general convex loss functions ϕ (i.e., generalized tensor completion) were initially studied by [1, 67] and [20], respectively. We apply tensor completion to fit a CP decomposition to a partially-observed tensor representing benchmark execution times by minimizing both least-squares and general convex loss functions. We leave exploration of alternative tensor decompositions to future work.

4.2 Optimization Methods

Both exact and approximate CP decomposition of fully- or partially-observed tensors is an NP hard problem [16]. We summarize numerical methods for tensor completion that minimize Equation 3 instantiated with various loss functions ϕ and any tensor order $d \geq 3$.

4.2.1 Least-squares loss. Methods for tensor completion typically fit a CP decomposition to a partially-observed tensor by minimizing Equation 3 with the least-squares loss function $\phi(t_{i_1, i_2, i_3}, \hat{t}_{i_1, i_2, i_3}) = (t_{i_1, i_2, i_3} - \hat{t}_{i_1, i_2, i_3})^2$. The Levenberg-Marquardt method and the alternating least-squares method (ALS) were the first methods proposed and evaluated for this problem by [67] and [1], respectively. ALS, which we use in Section 5.2, sweeps over the rows of each factor matrix, fixing the elements of all but one and minimizing, over the i_1 'th row of U, the objective

$$g(\mathbf{u}_{i_1}) = \frac{1}{|\Omega_{i_1}|} \left[\sum_{(i_2, i_3) \in \Omega_{i_1}} (t_{i_1, i_2, i_3} - \hat{t}_{i_1, i_2, i_3})^2 \right] + \lambda \|\mathbf{u}_{i_1}\|_2^2,$$

where $(i_2, i_3) \in \Omega_{i_1}$ if and only if $(i_1, i_2, i_3) \in \Omega$. Minimization of each row-wise convex objective involves solving a linear least-squares problem. The total arithmetic complexity of ALS is $O((\sum_{j=1}^d I_j)R^3 + |\Omega|dR^2)$ [56]. This overhead may be circumvented by optimizing factor matrix elements individually. In particular, the cyclic coordinate descent method (CCD), which was first proposed by [55] and later by [25] to enhance scalability in distributed-memory settings, minimizes the scalar objective $g(u_{i,r})$ and thereby reduces the arithmetic complexity of ALS by a factor of R . Both ALS and CCD achieve monotonic convergence, yet CCD often exhibits slower convergence due to its decoupling of row-wise factor matrix updates. Stochastic gradient descent instead iteratively updates all factor matrix elements at once and calculates the partial derivative of the corresponding objective using a random subset of observations within Ω . The efficiency of each method has been explored for tensor completion in both shared and distributed-memory settings [57].

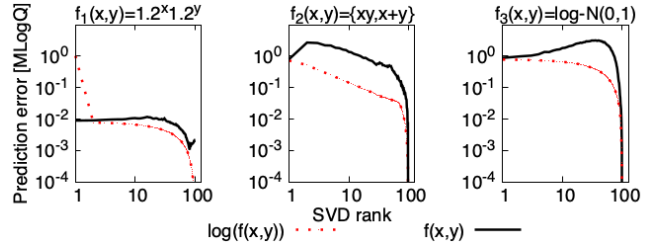


Figure 1: Singular value decompositions of three discretized functions evaluated for $1 \leq x, y \leq 100$. The two behaviors of f_2 are split along $x+y \leq 100$. Each element of f_1, f_2 is multiplied by $(1+N(0, .01))$, where $N(\mu, \sigma)$ denotes a sample from a normal distribution.

4.2.2 Generalized loss functions. Tensor completion may fit CP decompositions to partially-observed tensors by minimizing alternative loss functions [20]. These loss functions often indirectly apply constraints to elements within factor matrices (e.g., non-negativity), which are enforced by incorporating additional terms (e.g., penalty and barrier functions) into the objective. Alternating minimization and coordinate minimization may apply Newton's method to optimize row-wise and scalar nonlinear subproblems, respectively. In particular, alternating minimization via Newton's method (AMN) updates initial row-vector iterates $\mathbf{u}_{i_1}^{(0)}$ as follows until convergence:

$$\mathbf{u}_{i_1}^{(l+1)} \leftarrow \mathbf{u}_{i_1}^{(l)} - \mathbf{H}_f^{-1}(\mathbf{u}_{i_1}^{(l)}) \nabla g(\mathbf{u}_{i_1}^{(l)}), \quad (4)$$

where $\nabla g(\mathbf{u}_{i_1}^{(l)}) = \sum_{(i_2, i_3) \in \Omega_{i_1}} \nabla \phi(\mathbf{u}_{i_1}^{(l)}) + 2\lambda \mathbf{u}_{i_1}^{(l)}, \mathbf{H}_f(\mathbf{u}_{i_1}^{(l)}) = \sum_{(i_2, i_3) \in \Omega_{i_1}} \mathbf{H}_\phi(\mathbf{u}_{i_1}^{(l)}) + 2\lambda I$, and $\mathbf{H}_f, \mathbf{H}_\phi$ are Hessian matrices. Gradient-based methods such as stochastic gradient descent and L-BFGS have also been proposed [20], as have Gauss-Newton and quasi-Newton methods that optimize all factor matrices with each iteration [56].

We apply generalized tensor completion in Section 5.3 to achieve positive factor matrices by minimizing the MLogQ2 error metric (see Section 2.2). We append Equation 3 with log barrier functions applied element-wise to each factor matrix; each term is scaled by barrier parameter η . We then adapt the AMN method to solve a sequence of row-wise subproblems following Equation 4, each for a fixed value η , and decrease η geometrically until it is smaller than regularization parameter λ . This procedure follows established interior-point methods for nonlinear optimization [69].

5 APPLICATION PERFORMANCE MODELING VIA TENSOR COMPLETION

We apply tensor completion to optimize a low-rank canonical-polyadic (CP) decomposition of a tensor representation of an application's execution time. Our modeling framework enables user-specified partitioning of the modeling domain and provides loss functions to minimize user-specified error metrics. We formulate our approach to address the modeling problem described in Section 2.1.

5.1 Tensor Model Formulation

We use a tensor \mathcal{T} with d dimensions to model execution times of an application with d benchmark parameters. Each parameter corresponds to a distinct dimension (mode) of the tensor. For parameters

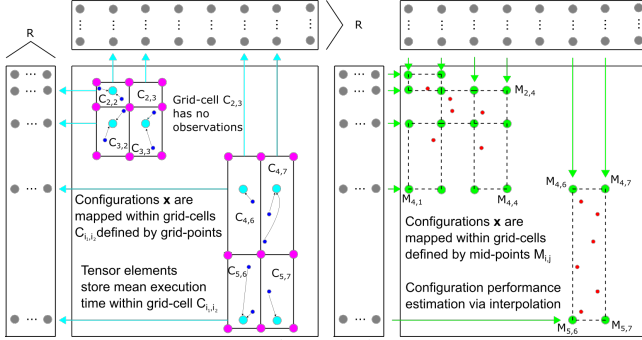


Figure 2: Training/inference (left/right) using a rank- R CP decomposition. ●. Tensor elements ● store the sample mean performance of intra-cell training configurations ●. ●. Interpolation of approximate tensor elements ● models performance of test configurations ●.

j with numerical values (e.g., matrix dimension), we discretize a subset of its range $\tilde{X}^{(j)} \subseteq X^{(j)}$ into I_j sub-intervals defined by parameter values $\tilde{X}_0^{(j)}, \tilde{X}_1^{(j)}, \dots, \tilde{X}_{I_j}^{(j)}$ using uniform or logarithmic spacing. In the case of categorical parameters, we simply index the choices along the corresponding tensor dimension. We then define a grid/tensor whose grid-points/entries are associated with the tensor product of both mid-points and end-points of each numerical parameter sub-interval, and distinct choices of each categorical parameter. As interpolation is not relevant along tensor modes corresponding to categorical parameters, we hereafter formulate our tensor model by solely considering numerical parameters.

For d -parameter configurations, tensor element $t_{i_1, \dots, i_d} \in \mathcal{T}$ is associated with the mid-points of a tensor product of sub-intervals $[\tilde{X}_{i_1}^{(1)}, \tilde{X}_{i_1+1}^{(1)}], \dots, [\tilde{X}_{i_d}^{(d)}, \tilde{X}_{i_d+1}^{(d)}]$. These bounding values define a grid-cell C_{i_1, \dots, i_d} with mid-point $(M_{i_1}^{(1)}, \dots, M_{i_d}^{(d)})$, which we associate with element t_{i_1, \dots, i_d} . If the j 'th parameter is discretized with logarithmic spacing, the mid-point of any sub-interval is given by $M_{i_j}^{(j)} = \lceil e^{(\log(X_{i_j}^{(j)}) + \log(X_{i_j+1}^{(j)}))/2} \rceil$. Given a set of executed configurations, t_{i_1, \dots, i_d} stores the mean execution time among those mapped within cell C_{i_1, \dots, i_d} . We leave evaluation of alternative quadrature schemes for future work.

Estimates are available for all tensor elements following completion of the tensor. We therefore use linear interpolation to predict execution times for arbitrary configurations $x \in \tilde{\mathcal{X}}$. Given such a configuration, let $\hat{t}_i \equiv \hat{t}_{i_1, \dots, i_d}$ be an estimate of the tensor element t_i associated with the grid-point $M_i \equiv (M_{i_1}^{(1)}, \dots, M_{i_d}^{(d)})$ just below x , so each $x_j \in [M_{i_j}^{(j)}, M_{i_j+1}^{(j)}]$. Then, using $h_j(x) = x$ for uniformly and $h_j(x) = \log(x)$ for logarithmically discretized parameter j , linear interpolation of neighboring tensor elements gives the execution time prediction,

$$\sum_{\mathbf{a} \in \{0,1\}^d} \hat{t}_{i+\mathbf{a}} \cdot \prod_{j=1}^d \left(1 - \frac{|h_j(x_j) - h_j(M_{i+\mathbf{a}}^{(j)})|}{h_j(M_{i+\mathbf{e}_j}^{(j)}) - h_j(M_i^{(j)})} \right). \quad (5)$$

If $x_j \in [X_0^{(j)}, M_0^{(j)}]$ or $x_j \in [M_{I_j-1}^{(j)}, X_{I_j}^{(j)}]$, we instead apply linear extrapolation along the j 'th mode using the corresponding values. If $x_j \notin [X_0^{(j)}, X_{I_j}^{(j)}]$ and thus $x \notin \tilde{\mathcal{X}}$, we forgo both interpolation

and linear extrapolation along the j 'th mode and instead propose an alternative technique for the estimation of tensor elements, which we describe in Section 5.3.

The selection of grid-spacing and sub-interval size along each dimension should facilitate accurate compression of tensor \mathcal{T} with small CP rank. Our modeling framework therefore enables user-directed domain discretization via specification of uniform or logarithmic to balance interpolation error and low-rank approximation error. We next describe two techniques to attain estimates for all elements of tensor \mathcal{T} via low-rank CP decomposition. Each targets scale-independent minimization of prediction error across the modeling domain as described in Section 2.2.

5.2 CP Decomposition Model Formulation for Interpolation

We describe a technique to optimize a low-rank CP decomposition of our tensor model that is both accurate and efficient in the interpolation setting described in Section 2.1. First, we transform observed entries to enable the use of a loss function that applies the MSE aggregate error metric, which we find is most efficient and least susceptible to round-off error among all error metrics summarized in Section 2.2. Specifically, we minimize Equation 3 with $\phi(t_i, \hat{t}_i) = (\log(t_i) - \hat{t}_i)^2$ using the ALS method described in Section 4.2.1. This simple technique minimizes deviation in the scale of observed execution times and thereby enhances the robustness of MSE to both noise and biased under/over-prediction. This is observed in Figure 1 using singular value decompositions (SVD), which minimize $\sqrt{\text{MSE}}$. In particular, the log-transformed matrices achieve a monotonic decrease in MLogQ prediction error with increasing SVD rank, whereas the same error metric can increase with increasing SVD rank for untransformed matrices. We assign non-positive entries a value 10^{-16} prior to evaluation of MLogQ for all matrices in Figure 1.

Use of logarithmic transformations attains non-negative CP decomposition model output implicitly without the requisite constraints to enforce non-negativity in factor matrix elements. The resulting model approximates the execution time $f(\mathbf{x})$ of configuration \mathbf{x} as

$$m(\mathbf{x}) = \sum_{\mathbf{a} \in \{0,1\}^d} e^{\hat{t}_{i+\mathbf{a}}} \cdot \prod_{j=1}^d \left(1 - \frac{|\log(x_j) - \log(M_{i+\mathbf{a}}^{(j)})|}{\log(M_{i+\mathbf{e}_j}^{(j)}) - \log(M_i^{(j)})} \right),$$

where $M_i^{(j)} \leq x_j < M_{i+\mathbf{e}_j}^{(j)}, \forall j \in \{1, \dots, d\}$. As mentioned in Section 5.1, if $x_j \in [X_0^{(j)}, M_0^{(j)}]$ or $x_j \in [M_{I_j-1}^{(j)}, X_{I_j}^{(j)}]$, we instead apply linear extrapolation along the j 'th mode using the corresponding values. We summarize training and inference in an interpolation setting across a two-dimensional domain in Figure 2.

5.3 CP Decomposition Model Formulation for Extrapolation

We next describe a technique to optimize a low-rank CP decomposition of our tensor model that enables inference in the extrapolation setting described in Section 2.1. A CP decomposition (e.g., that formulated in Section 5.2), appears difficult to use in this setting, as one must predict unseen rows of its factor matrices, which may lack

Library	Application [parameter description]	Input	Architectural	Configuration
ExaFMM[72]	Fast multipole method [number of particles per node n , expansion order ord , particles per leaf ppl , partitioning tree level tl]	$2^{12} \leq n \leq 2^{16}$, $4 \leq ord \leq 15$	$1 \leq tpp \leq 64$, $1 \leq ppn \leq 64$	$32 \leq ppl \leq 256$, $0 \leq tl \leq 4$
AMG[53]	Algebraic multigrid [Problem size per process $nx/ny/nz$, coarsening/relaxation/interpolator type $ct/rt/it$]	$2^3 \leq nx, ny, nz \leq 2^7$	$1 \leq tpp \leq 64$, $1 \leq ppn \leq 64$	$ct \in \{0, 3, 6, 8, 10, 21, 22\}$, $rt \in \{0, 3, 4, 6, 8, 13, 14, 16, 17, 18\}$, $it \in \{0, 2, 3, 4, 5, 6, 8, 9, 12, 13, 14, 16, 17, 18\}$
KRIPKE[30]	Discrete ordinates transport [$groups$, $legendre$, $quad$, $dset$, $gset$, layout l , solver s]	$2^3 \leq groups \leq 2^7$, $0 \leq legendre \leq 5$, $2^3 \leq quad \leq 2^7$	$1 \leq tpp \leq 64$, $1 \leq ppn \leq 64$	$l \in \{dgz, dzg, gdz, gzd, zdg, zgd\}$, $s \in \{sweep, bj\}$, $8 \leq dset \leq 64$, $1 \leq gset \leq 32$

Table 2: Parameter space description for algebraic multigrid and multiple parallel scientific applications. Parameters N , ppn and tpp refer to node count, processes-per-node and threads-per-process under the constraint that $64 \leq ppn \cdot tpp \leq 128$.

structure due to cancellation of its positive and negative elements. However, a rank-1 CP decomposition exhibits structure naturally, as performance typically increases or decreases monotonically as the value of a numerical parameter increases. One can then simply extrapolate a sequence using line-fitting techniques. To retain accuracy in CP factor matrices that correspond to parameters that are not being extrapolated, we do not restrict CP rank to 1 and instead apply rank-1 factorizations to strictly positive factor matrices. We then apply line-fitting to extrapolate each rank-1 factorization.

We utilize the generalized tensor completion framework summarized in Section 4.2.2 to ensure positive factor matrices. Specifically, we minimize Equation 3 with loss function $\phi(t_i, \hat{t}_i) = (\log(t_i) - \log(\hat{t}_i))^2$ using the interior-point method described in Section 4.2.2. We then leverage the Perron-Frobenius theorem, which states that the best rank-1 approximation to a strictly positive matrix is itself positive, ensuring positive predictions. While positive factor matrices attained in this way are not typically low-rank, we find empirically that this technique retains sufficient accuracy because the low-rank approximation error does not compromise the contributions from other factor matrices when estimating a tensor element. We leave evaluation of alternative schemes to enable robust extrapolation using a CP decomposition for future work.

We fit a univariate spline model to the positive left singular vector of each factor matrix corresponding to a numerical or architectural benchmark parameter. In particular, we use elements of this vector as a training set, which we log-transform element-wise, to configure a MARS model, which we summarized in Section 3.2. Thus, for $d = 3$ yet without loss of generality, when presented a configuration $\mathbf{x} \notin \tilde{\mathcal{X}}$ such that $x_1 \notin [X_0^{(1)}, X_{I_1}^{(1)}]$, $x_2 \in [X_0^{(2)}, X_{I_2}^{(2)}]$, $x_3 \in [X_0^{(3)}, X_{I_3}^{(3)}]$ we modify Equation 2 by estimating tensor element t_i as

$$\hat{t}_i = \sum_{r=1}^R e^{\hat{m}(\log(x_1))} \hat{\sigma} \hat{v}_r v_{i_2, r} w_{i_3, r},$$

where $\mathbf{U} \approx \hat{\mathbf{u}}\hat{\sigma}\hat{\mathbf{v}}^T$ and $\hat{m} : \mathbb{R} \rightarrow \mathbb{R}$ is the spline model configured by MARS using training set $\log(\hat{\mathbf{u}})$. In a general setting with $d \geq 2$, when presented with a configuration $\mathbf{x} \notin \tilde{\mathcal{X}}$ such that interpolation is invoked along at least one numerical benchmark parameter (i.e., $\exists j$ s.t. $x_j \in [X_0^{(j)}, X_{I_j}^{(j)}]$), we utilize Equation 5 to approximate execution time $f(\mathbf{x})$ and treat extrapolated numerical parameters as we do categorical (i.e., no interpolation along its tensor dimension).

6 EXPERIMENTAL METHODOLOGY

6.0.1 Machine. We use the Stampede2 supercomputer at Texas Advanced Computing Center (TACC)[61]. Stampede2 consists of 4200 Intel Knights Landing (KNL) compute nodes, each connected by an Intel Omni-Path (OPA) network with a fat-tree topology. Each KNL compute node provides 68 cores with 4 hardware threads per core. We use Intel environment 18.0.2, Intel MPI environment 18.0.2, and corresponding icc, mpicc, and mpicxx compilers. We generate all models sequentially.

6.0.2 Application Libraries. We execute Intel MKL’s GEMM (MM) routine $C_{m \times n} \leftarrow A_{m \times k} B_{k \times n} + \beta C_{m \times n}$ in a single-threaded environment with matrix dimensions $32 \leq m, n, k \leq 4096$. We execute Intel MKL’s GEQRF (QR) routine $A_{m \times n} \leftarrow \alpha Q_{m \times n} R_{n \times n}$ in a single-threaded environment with matrix dimensions $32 \leq m, n \leq 262144$ such that $m \geq n$ and all three matrices fit in memory. We execute Intel MPI’s Broadcast (BC) routine on $\{1, 2, 4, 8, 16, 32, 64, 128\}$ nodes with $\{1, 2, 4, 8, 16, 32, 64\}$ processes-per-node (ppn), and message size $2^{16} \leq m \leq 2^{26}$. ExaFMM[72] is an open source library for fast multipole methods aimed towards exascale systems. AMG[53] is a parallel algebraic multigrid solver for linear systems arising from problems on unstructured grids. Kripke [30] is a proxy application for modern discrete ordinates neutral particle transport applications. We execute each application configuration on a single-node, and model the execution times of the $m2l_p2p$ kernel for ExaFMM and the total solve time for AMG and Kripke. Table 2 details each application’s parameter space.

6.0.3 Dataset Generation. To optimize and evaluate performance models, we generate training sets and test sets for each kernel and application. Individual configurations within both sets are formulated using distinct sampling strategies for distinct parameter types. In particular, the specified ranges of both input parameters (e.g., matrix dimension, message size) and architectural parameters (e.g., node count, ppn) are sampled log-uniformly at random, while the ranges of each configuration parameter (e.g., block size) are sampled uniformly at random. The test sets for matrix multiplication, QR factorization, MPI broadcast, ExaFMM, AMG, and Kripke feature 1000, 1000, 10484, 2512, 21534, and 8745 configurations, respectively. Each kernel configuration is executed 50x or until the coefficient of variation of its corresponding execution time is < 0.01 . Each application configuration is executed once.

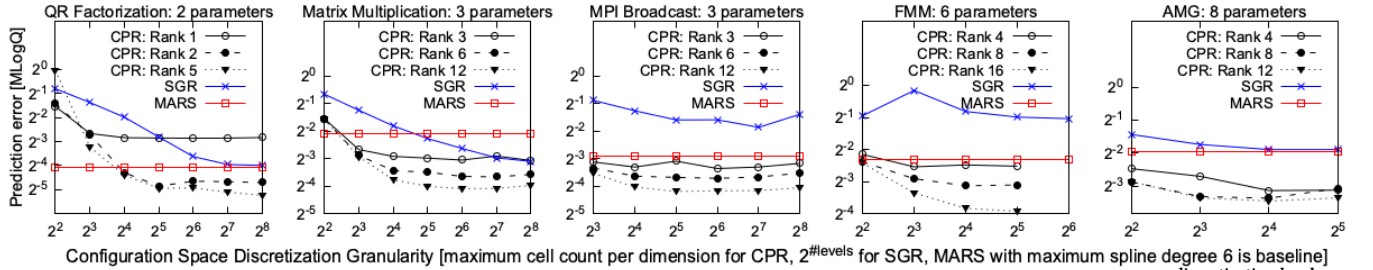


Figure 3: Prediction accuracy for grid-based models. Discretization granularity signifies the number of cells for CPR and $2^{\text{discretization level}}$ for SGR. The training-set sizes for each kernel/application are $2^{16}, 2^{16}, 2^{15}, 2^{15}, 2^{14}$, respectively.

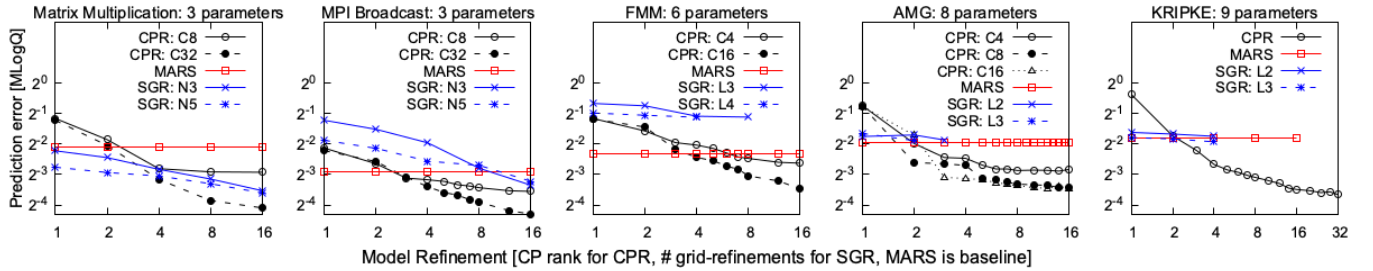


Figure 4: Prediction accuracy for grid-based models following refinement of initial model (CP rank for CPR, sparse grid for SGR). C_k and L_k denote cell count and sparse grid-level k , respectively. The training-set sizes for each kernel/application are $2^{16}, 2^{15}, 2^{15}, 2^{14}, 2^{14}$, respectively.

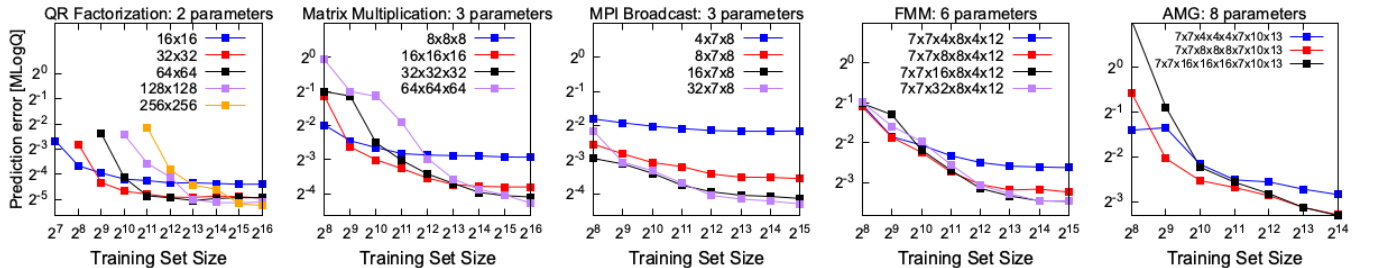


Figure 5: Prediction accuracy for the CPR model. Tensors corresponding to each CPR model becomes increasingly dense with increasing training set size. For each tensor, the minimal prediction error across CP ranks is reported.

6.0.4 Model Tuning and Evaluation. We evaluate the following prediction methods: sparse grid regression (SGR), multi-layer perceptrons (NN), random forests (RF), gradient-boosting (GB), extremely-randomized trees (ET), Gaussian process regression (GP), support vector machines (SVM), adaptive spline regression (MARS), k-nearest neighbors (KNN), and our methodology described in Section 5 (CPR). We optimize these models using a random sample from each training set and log-transform execution times and application parameters. Results for SVM, RF, and GB are not provided in Figures 6, 7, and 8 because each attains a strictly less accurate model than others of the same model class: GP and ET, respectively.

We utilize the Cyclops Tensor Framework [59] for efficient CP decomposition optimization. We utilize the PyEarth library to evaluate MARS, the SG++ [50] library to evaluate SGR, and the Scikit-Learn [48] library to evaluate the remaining methods. We evaluate all relevant model configurations using the same training

set and forgo training via cross-validation. In particular, we evaluate CP ranks $1 \rightarrow 64$ and grid-cell counts $4 \rightarrow 256$ per dimension for CPR; discretization levels $2 \rightarrow 8, 1 \rightarrow 16$ refinements, and $4 \rightarrow 32$ adaptive grid-points for SGR; max spline degrees of $1 \rightarrow 6$ for MARS; max tree depths of $2 \rightarrow 16$ and max tree counts of $1 \rightarrow 64$ for RFR, GBR, and ETR; $1 \rightarrow 6$ neighbors for KNN, {RationalQuadratic,RBF,DotProduct+WhiteKernel, Matern,ConstantKernel} covariance kernels for GPR; {poly,rbf} kernels and polynomial degrees $1 \rightarrow 3$ for SVM; $1 \rightarrow 8$ hidden layers each of size $2 \rightarrow 2048$ and {relu,tanh} activation functions for NN.

CPR places grid-points equally-spaced on a log-scale/linear-scale along the ranges of input/architectural/configuration parameters, and interpolates as necessary. We select regularization parameter $\lambda = 10^{-k}, \forall k \in \{-6, \dots, -3\}$ for CPR and SGR. We set a maximum number of 100 sweeps and 1000 iterations of alternating least-squares and conjugate gradient for CPR and SGR, respectively, and set a tolerance of 10^{-4} for SGR. We initialize the barrier parameter η for extrapolation experiments using CPR to 10 and decrease

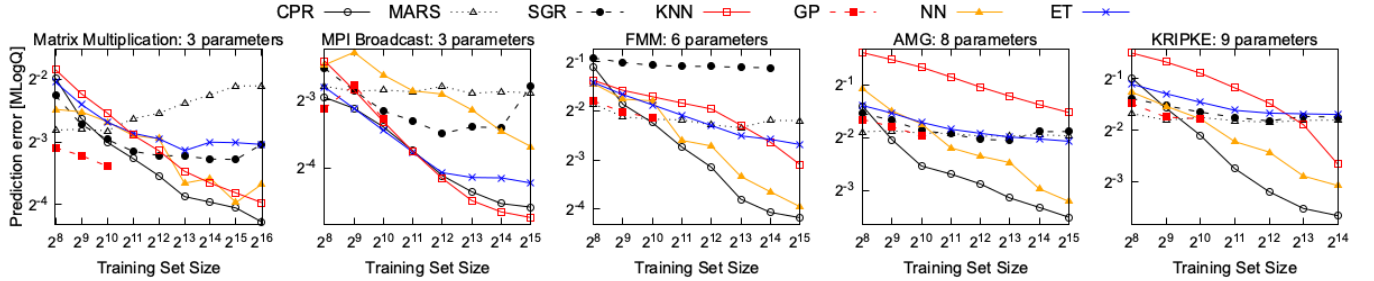


Figure 6: Prediction error for grid-based models and alternative supervised learning models as a function of training set size. Each datapoint represents the minimum error achieved by exhaustively exploring the corresponding model’s hyper-parameters as described in Section 6.0.4.

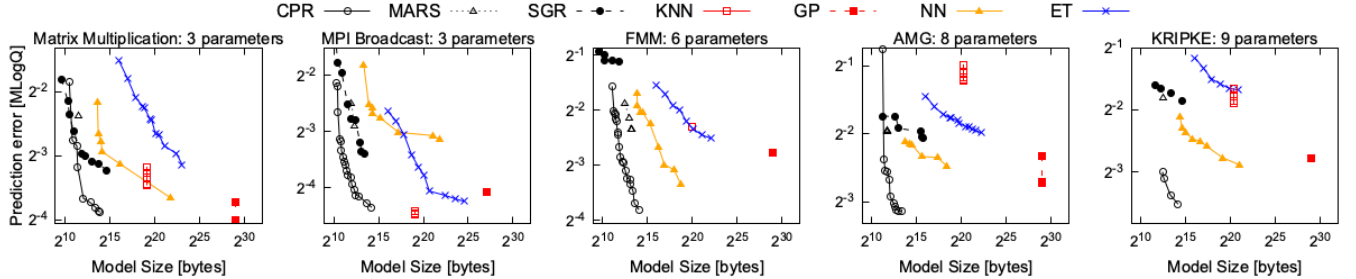


Figure 7: Prediction error for grid-based models and alternative supervised learning models as a function of model size. The complexity of each model is varied by evaluating all hyper-parameters as described in Section 6.0.4. All models are trained using 8192 samples.

geometrically by a factor of 8 until $\eta \leq 10^{-11}$. In these experiments, we set a maximum of 40 iterations of Newtons method to solve each row-wise optimization problem for a fixed value η .

We assess model prediction error on test configurations using the MLogQ error metric as detailed in Section 2.2. We assess model size by writing performance models optimized for the interpolation setting described in Section 2.1 to a file via Python’s *joblib* package and measuring file size. We forgo consideration of models optimized in ≥ 1000 seconds in Figures 6 and 7, or models of size ≥ 10 megabytes in Figure 6. As our focus is on evaluating model accuracy, we forgo consideration of model evaluation latency and training time.

7 EXPERIMENTAL EVALUATION

We evaluate each class of performance models generated by methods described in Section 3 and specified in Section 6.0.4. Following the methodology proposed in Section 2.2, we first assess piecewise/grid-based models and alternative supervised learning methods for the interpolation problem described in Section 2.1. We then assess each class of models for both single-parameter and multi-parameter extrapolation also described in that section. We provide Python scripts² to reproduce all experiments summarized in Figures 3, 4, 5, 6, 7, and 8.

7.1 Model Evaluation for Interpolation

Existing piecewise/grid-based performance models exhibit fundamental trade-offs between accuracy and scalability. Each metric is significantly influenced by discretization geometry (i.e., location of grid-points) and granularity (i.e., number of grid-points dictated by

discretization geometry) across the modeling domain. Both influence the observation density within individual grid-cells for a fixed training set. We evaluate prediction error in the interpolation setting described in Section 2.1 across varying domain discretization and grid refinement strategies. We then incorporate alternative supervised learning methods to compare model accuracy as a function of model size and number of training observations.

7.1.1 Prediction Accuracy vs. Domain Discretization. We observe in Figure 3 that compression of high-dimensional regular grids via CP decomposition (CPR) facilitates higher model prediction accuracy than regression across high-dimensional sparse grids (SGR). Figure 3 further demonstrates that given sufficiently many training observations, CPR alone among piecewise/grid-based models systematically improves model accuracy by independently varying the discretization granularity along the ranges of numerical parameters across all five benchmarks. We remark that when applications feature both numerical and integer/categorical parameters, user-controlled discretization of the modeling domain, which CPR alone facilitates, is critical to formulating an accurate performance model. As observed for the FMM and AMG benchmarks in Figure 3, each of which features both types of parameters, SGR’s strategy of varying the discretization granularity across all dimensions simultaneously offers no improvement in prediction accuracy. Discretization geometry selected via search alone (MARS) configures global models that are significantly less accurate than CPR. For both high-dimensional benchmarks, this enables CPR to achieve up to 4x improvements in mean prediction accuracy over SGR and MARS.

Figure 3 highlights that use of a regular grid, as opposed to alternatives such as a sparse grid, is most conducive to systematic improvement in model prediction accuracy. However, our approach,

²<https://github.com/huttered40/cpr-perf-model/tree/main/reproducibility>

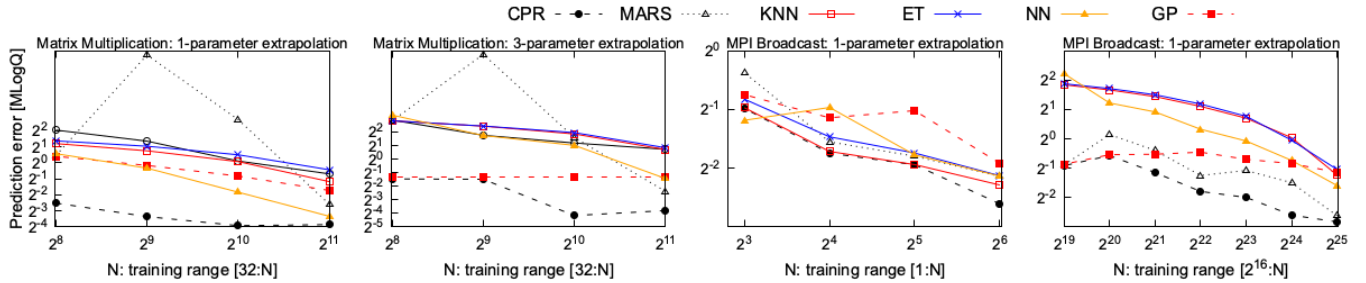


Figure 8: Extrapolation error for configurations beyond the specified training ranges of matrix dimension m and all matrix dimensions for Matrix Multiplication, and on node count and message size for MPI Broadcast, respectively. All models are trained using 4096 samples.

CPR, is the only available technique to achieve a scalable representation of such a grid for a high-dimensional modeling domain. Results in Figures 3 and 4 show that explicit use of a regular grid isn't necessary; even a rank-4 CP decomposition model of its corresponding tensor representation is sufficient to achieve higher accuracy than that attained by SGR and MARS. Further, the prediction accuracy of CPR continues to improve for a fixed CP rank even as the underlying tensors become increasingly sparse.

Results in Figure 4 indicate that CP rank offers the most accurate and efficient mechanism for improving prediction accuracy among those provided by piecewise/grid-based models. We observe that as tensor models grow in size, a higher CP rank is needed to leverage the finer discretization of the underlying regular grid. However, up to 4x improvements in prediction accuracy are achieved even with CP rank-8 models for the largest evaluated tensors. SGR instead refines its underlying sparse grid, each sweep iterating over training data to identify grid-points and corresponding basis functions contributing most to training error. The discretization geometry around those grid-points is modified before restarting the procedure on the newly refined grid. As observed in Figure 4, even with up to 16 grid-refinements (which can take more than 1000 seconds), sparse grid models cannot achieve prediction accuracy competitive with CPR, which does not refine its underlying grid.

7.1.2 Prediction Accuracy vs. Training Set Size. We observe in Figure 5 that CPR improves mean prediction accuracy with increasingly fine regular grids only if the corresponding tensor is sufficiently dense. Notably, as the number of benchmark parameters increases, the requisite tensor density to optimize an accurate low-rank CP decomposition model decreases. In particular, for MM, a 32x32x32 tensor model offers best prediction accuracy when at least 50% dense (training set size of 2^{14}), whereas for AMG, a 7x7x8x8x8x7x10x13 tensor model is 0.07% dense yet most accurate at the same training set size. Thus, the size of the training set, along with tensor size, is most indicative of the accuracy these models can attain.

We tune over the optimal tensor size and CP rank in Figure 6, which further shows systematic improvements in prediction accuracy with increasingly large training sets. CPR achieves the highest prediction accuracy among alternative models using increasingly large training sets of applications FMM, AMG, and KRIKE in Figure 6. Neural networks are most competitive among alternative models for modeling performance across high-dimensional domains. We further observe that accurate CPR models can be optimized

with small training sets using small tensors and moderate CP rank. However, alternative models are more competitive in this regime, indicating that CPR is most effective relative to the state-of-the-art for training sets of moderate to large size.

7.1.3 Prediction Accuracy vs. Model Size. We observe in Figure 7 that CPR models achieve the highest prediction accuracy relative to model size among alternative models for all five benchmarks. Improvement in this metric is also observed as the number of application benchmark parameters increases for a fixed-size training set. In particular, CPR approximately matches KNN and GP methods in prediction accuracy for the MM and BC kernels, despite using 16384x and 32x less memory, respectively. For FMM, AMG, and KRIKE, the execution times of which depend on at least six parameters, CPR achieves the smallest prediction error outright, and uses 50x less memory than the most accurate neural network model.

Among piecewise/grid-based models, CPR decouples discretization granularity of the modeling domain from model size if performance across its underlying grids is sufficiently low-rank. This is attributed to properties characteristic to CP decomposition and listed in Section 3.2. Namely, as the number of benchmark parameters increases (a segment of a general trend), the CPD model size grows linearly with tensor order for a fixed rank and tensor size. Thus, memory-efficiency is retained even when modeling performance across high-dimensional domains, as we observe in Figure 7. Fully-connected neural networks, the size of which scales linearly in number of layers, are most competitive with CPR among alternative supervised learning methods for large training sets. For all evaluated benchmarks, alternative piecewise/grid-based models (e.g., MARS), while competitive with CPR in model size, cannot fit to complex performance data as accurately using sparse grids or high-degree splines. Instance-based methods (e.g., KNN) achieve increasingly poor accuracy in higher dimensions due to increasingly sparse observation of the modeling domain. Highly tuned kernel-based methods (e.g., GP) and recursive partitioning methods (e.g., ET) require an exorbitant memory requirement, yet achieve increasingly poor accuracy in higher dimensions.

7.2 Model Evaluation for Extrapolation

We assess all models for both single-parameter and multi-parameter extrapolation using the matrix multiplication (MM) and MPI broadcast (BC) kernels. For each kernel, we select a subset of its numerical or integer parameters and assign the corresponding multi-parameter configurations to a training set or test set according to

the magnitudes of the selected parameters. Specifically, the test sets for MM consist of all configurations $(m, n, k) : 2048 \leq m \leq 4096$ and all configurations $(m, n, k) : 2048 \leq m, n, k \leq 4096$, while the corresponding training sets consist of all configurations $(m, n, k) : 32 \leq m < N$ and all configurations $(m, n, k) : 32 \leq m, n, k < N$ for $2^8 \leq N \leq 2^{11}$, respectively. The test sets for BC consist of all configurations executed with 128 nodes and all message sizes $m : 2^{25} \leq m \leq 2^{26}$, while the corresponding training sets consist of all configurations executed with node counts $p : 1 \leq p \leq N$ for $8 \leq N \leq 64$ and all message sizes $m : 2^{16} \leq m < N$ for $2^{19} \leq N \leq 2^{25}$, respectively. As we have already ablated these models for the interpolation setting, we randomly select 4096 samples from each training set and report the most accurate model as N is decreased geometrically.

We observe in Figure 8 that our approach, CPR, is significantly more accurate than alternative models when extrapolating numerical parameters of MM and BC kernels. All alternative models we evaluate overfit to training observations irrespective of model complexity. CPR instead captures monotonically increasing performance behavior observed within training observations along the columns of each corresponding factor matrix to enhance extrapolation accuracy. CPR also benefits from user-directed discretization granularity along the dimensions corresponding to extrapolated parameters, as a finer discretization (i.e., larger tensor dimension) enables use of a larger training set to improve optimization of spline models as described in Section 5.3. As N decreases and observed performance behavior among training configurations along factor matrices is less predictive of performance within test set configurations, CPR's extrapolation error increases accordingly. However, when extrapolating a single numerical parameter for both MM and BC kernels, CPR is consistently more accurate as N decreases by 8x and 2x, respectively.

Our model is less accurate when extrapolating integer parameters, which we observe when extrapolating node count for the BC kernel in Figure 8. This can be attributed to the small training set with which the spline model of the corresponding factor matrix's left singular vector is optimized, as well as non-monotonic performance behavior that CPR captures which is characteristic to smaller-scale experiments but not to larger-scale. In particular, for this kernel and $N \leq 32$, CPR matches KNN in achieving 25% mean prediction error. Overall, these results suggest that if performance behavior of moderate-dimension kernels at small-scale is conducive to that at large-scale, our methodology described in Section 5.3 is relatively well-equipped to extrapolate performance accurately.

8 CONCLUSION

Our experimental analysis demonstrates that a CP decomposition can accurately and efficiently model application performance across high-dimensional parameter spaces. These models are significantly more accurate than alternative models relative to model size (and increasingly so as the number of benchmark parameters increases), and systematically reduce prediction error given increasingly many observations of a fixed modeling domain. The impetus for tensor completion driven by artificial intelligence (e.g., recommendation systems, image recognition) ensures that performance modeling

frameworks that adopt this technique will benefit from its continued optimization and dissemination among software libraries.

This work presents promising avenues for autotuning research involving the use of tensor factorizations as surrogate models of application performance. Remaining challenges using tensor completion in this setting include handling performance observation datasets with different (non-random) structure that reflects exploration and exploitation sampling methods and/or highly-constrained parameter spaces, as well as incorporating methods for efficiently updating CP decompositions to effectively model streaming data in online settings [26, 42, 60]. An additional gap in our evaluation for this setting includes optimization of tensor factorizations to target accurate identification of fast configurations (e.g., that proposed in [41]) as opposed to minimizing prediction error over all configurations in aggregate.

ACKNOWLEDGMENTS

The first author would like to acknowledge the Department of Energy (DOE) and Krell Institute for support via the DOE Computational Science Graduate Fellowship (grant No. DE-SC0019323). This work used Stampede2 at the Texas Advanced Computing Center through allocation CCR180006 from the Advanced Cyberinfrastructure Coordination Ecosystem: Services & Support (ACCESS) program, which is supported by National Science Foundation grants #2138259, #2138286, #2138307, #2137603, and #2138296. This research has also been supported by funding from the National Science Foundation via grant #1942995.

REFERENCES

- [1] Evrim Acar, Daniel M Dunlavy, Tamara G Kolda, and Morten Mørup. 2011. Scalable tensor factorizations for incomplete data. *Chemometrics and Intelligent Laboratory Systems* 106, 1 (2011), 41–56.
- [2] Riyadh Baghdadi, Massinissa Merouani, Mohamed-Hicham Leghetta, Kamel Abdous, Taha Arbaoui, Karima Benatchba, et al. 2021. A deep learning based cost model for automatic code optimization. *Proceedings of Machine Learning and Systems* 3 (2021), 181–193.
- [3] Bradley J Barnes, Barry Rountree, David K Lowenthal, Jaxk Reeves, Bronis De Supinski, and Martin Schulz. 2008. A regression-based approach to scalability prediction. In *Proceedings of the 22nd annual international conference on Supercomputing*. 368–377.
- [4] Alexandru Calotoiu, David Beckinsale, Christopher W Earl, Torsten Hoefer, Ian Karlin, Martin Schulz, and Felix Wolf. 2016. Fast multi-parameter performance modeling. In *2016 IEEE International Conference on Cluster Computing (CLUSTER)*. IEEE, 172–181.
- [5] Alexandru Calotoiu, Torsten Hoefer, Marius Poke, and Felix Wolf. 2013. Using automated performance modeling to find scalability bugs in complex codes. In *Proceedings of the International Conference on High Performance Computing, Networking, Storage and Analysis*. 1–12.
- [6] Sai P Chenna, Greg Stitt, and Herman Lam. 2019. Multi-parameter performance modeling using symbolic regression. In *2019 International Conference on High Performance Computing & Simulation (HPCS)*. IEEE, 312–321.
- [7] Jaemin Choi, David F Richards, Laxmikant V Kale, and Abhinav Bhatele. 2020. End-to-end performance modeling of distributed GPU applications. In *Proceedings of the 34th ACM International Conference on Supercomputing*. 1–12.
- [8] Marcin Copik, Alexandru Calotoiu, Tobias Grosser, Nicolas Wicki, Felix Wolf, and Torsten Hoefer. 2021. Extracting clean performance models from tainted programs. In *Proceedings of the 26th ACM SIGPLAN Symposium on Principles and Practice of Parallel Programming*. 403–417.
- [9] Marc Courtois and Murray Woodside. 2000. Using regression splines for software performance analysis. In *Proceedings of the 2nd international workshop on Software and performance*. 105–114.
- [10] Dmitry Duplyakin, Jed Brown, and Robert Ricci. 2016. Active learning in performance analysis. In *2016 IEEE international conference on cluster computing (CLUSTER)*. IEEE, 182–191.
- [11] Jerome H Friedman. 1991. Multivariate adaptive regression splines. *The annals of statistics* (1991), 1–67.

- [12] Ryan D Friese, Nathan R Tallent, Abhinav Vishnu, Darren J Kerbyson, and Adolfy Hoisie. 2017. Generating performance models for irregular applications. In *2017 IEEE International Parallel and Distributed Processing Symposium (IPDPS)*. IEEE, 317–326.
- [13] Jochen Garske. 2012. Sparse grids in a nutshell. In *Sparse grids and applications*. Springer, 57–80.
- [14] Evangelos Georganas, Jorge González-Domínguez, Edgar Solomonik, Yili Zheng, Juan Tourino, and Katherine Yelick. 2012. Communication avoiding and overlapping for numerical linear algebra. In *SC'12: Proceedings of the International Conference on High Performance Computing, Networking, Storage and Analysis*. IEEE, 1–11.
- [15] Simon F Goldsmith, Alex S Aiken, and Daniel S Wilkerson. 2007. Measuring empirical computational complexity. In *Proceedings of the the 6th joint meeting of the European software engineering conference and the ACM SIGSOFT symposium on The foundations of software engineering*, 395–404.
- [16] Christopher J Hillar and Lek-Heng Lim. 2013. Most tensor problems are NP-hard. *Journal of the ACM (JACM)* 60, 6 (2013), 1–39.
- [17] Frank L Hitchcock. 1927. The expression of a tensor or a polyadic as a sum of products. *Journal of Mathematics and Physics* 6, 1–4 (1927), 164–189.
- [18] Torsten Hoefer, William Gropp, William Kramer, and Marc Snir. 2011. Performance modeling for systematic performance tuning. In *SC'11: Proceedings of 2011 International Conference for High Performance Computing, Networking, Storage and Analysis*. IEEE, 1–12.
- [19] Torsten Hoefer, William Gropp, Rajeev Thakur, and Jesper Larsson Träff. 2010. Toward performance models of MPI implementations for understanding application scaling issues. In *European MPI Users' Group Meeting*. Springer, 21–30.
- [20] David Hong, Tamara G Kolda, and Jed A Duersch. 2020. Generalized canonical polyadic tensor decomposition. *SIAM Rev.* 62, 1 (2020), 133–163.
- [21] Ling Huang, Jinzhu Jia, Bin Yu, Byung-Gon Chun, Petros Maniatis, and Mayur Naik. 2010. Predicting execution time of computer programs using sparse polynomial regression. *Advances in neural information processing systems* 23 (2010).
- [22] Huda Ibeid, Siping Meng, Oliver Dobon, Luke Olson, and William Gropp. 2019. Learning with analytical models. In *2019 IEEE International Parallel and Distributed Processing Symposium Workshops (IPDPSW)*. IEEE, 778–786.
- [23] Engin İpek, Sally A McKee, Rich Caruana, Bronis R de Supinski, and Martin Schulz. 2006. Efficiently exploring architectural design spaces via predictive modeling. *ACM SIGOPS Operating Systems Review* 40, 5 (2006), 195–206.
- [24] Nikhil Jain, Abhinav Bhatele, Michael P Robson, Todd Gamblin, and Laxmikant V Kale. 2013. Predicting application performance using supervised learning on communication features. In *Proceedings of the International Conference on High Performance Computing, Networking, Storage and Analysis*. 1–12.
- [25] Lars Karlsson, Daniel Kressner, and Andrzej Uschmajew. 2016. Parallel algorithms for tensor completion in the CP format. *Parallel Comput.* 57 (2016), 222–234.
- [26] Hiroyuki Kasai. 2016. Online low-rank tensor subspace tracking from incomplete data by CP decomposition using recursive least squares. In *2016 IEEE International Conference on Acoustics, Speech and Signal Processing (ICASSP)*. IEEE, 2519–2523.
- [27] Sam Kaufman, Phitchaya Phothilimthana, Yanqi Zhou, Charith Mendis, Sudip Roy, Amit Sabne, and Mike Burrows. 2021. A learned performance model for tensor processing units. *Proceedings of Machine Learning and Systems* 3 (2021), 387–400.
- [28] Darren J Kerbyson, Henry J Alme, Adolfy Hoisie, Fabrizio Petrini, Harvey J Wasserman, and Mike Gittings. 2001. Predictive performance and scalability modeling of a large-scale application. In *Proceedings of the 2001 ACM/IEEE conference on Supercomputing*, 37–37.
- [29] Tamara G Kolda and Brett W Bader. 2009. Tensor decompositions and applications. *SIAM review* 51, 3 (2009), 455–500.
- [30] Adam J Kunen, Teresa S Bailey, and Peter N Brown. 2015. *Kripke-a massively parallel transport mini-app*. Technical Report. Lawrence Livermore National Lab.(LLNL), Livermore, CA (United States).
- [31] Benjamin C Lee and David M Brooks. 2006. Accurate and efficient regression modeling for microarchitectural performance and power prediction. *ACM SIGOPS operating systems review* 40, 5 (2006), 185–194.
- [32] Benjamin C Lee, David M Brooks, Bronis R de Supinski, Martin Schulz, Karan Singh, and Sally A McKee. 2007. Methods of inference and learning for performance modeling of parallel applications. In *Proceedings of the 12th ACM SIGPLAN symposium on Principles and practice of parallel programming*, 249–258.
- [33] Rui Li, Aravind Sukumaran-Rajam, Richard Veras, Tze Meng Low, Fabrice Rastello, Atanas Rountev, and Ponnuswamy Sadayappan. 2019. Analytical cache modeling and tilesize optimization for tensor contractions. In *Proceedings of the International Conference for High Performance Computing, Networking, Storage and Analysis*. 1–13.
- [34] Rui Li, Yufan Xu, Aravind Sukumaran-Rajam, Atanas Rountev, and P. Sadayappan. 2021. Analytical Characterization and Design Space Exploration for Optimization of CNNs. In *Proceedings of the 26th ACM International Conference on Architectural Support for Programming Languages and Operating Systems (Virtual, USA) (ASPLOS 2021)*. Association for Computing Machinery, New York, NY, USA, 928–942. <https://doi.org/10.1145/3445814.3446759>
- [35] Ji Liu, Przemyslaw Musialski, Peter Wonka, and Jieping Ye. 2012. Tensor completion for estimating missing values in visual data. *IEEE transactions on pattern analysis and machine intelligence* 35, 1 (2012), 208–220.
- [36] Yang Liu, Wissam M Sid-Lakhdar, Osnir Marques, Xinran Zhu, Chang Meng, James W Demmel, and Xiaoye S Li. 2021. GPTune: multitask learning for autotuning exascale applications. In *Proceedings of the 26th ACM SIGPLAN Symposium on Principles and Practice of Parallel Programming*, 234–246.
- [37] Tze Meng Low, Francisco D. Igual, Tyler M. Smith, and Enrique S. Quintana-Ortí. 2016. Analytical Modeling Is Enough for High-Performance BLIS. *ACM Trans. Math. Softw.* 43, 2, Article 12 (aug 2016), 18 pages. <https://doi.org/10.1145/2925987>
- [38] Hengrui Luo, James W Demmel, Younghyun Cho, Xiaoye S Li, and Yang Liu. 2021. Non-smooth Bayesian optimization in tuning problems. *arXiv preprint arXiv:2109.07563* (2021).
- [39] Piotr Luszczek, Wissam M Sid-Lakhdar, and Jack Dongarra. 2023. Combining multitask and transfer learning with deep Gaussian processes for autotuning-based performance engineering. *The International Journal of High Performance Computing Applications* (2023), 10943420231166365.
- [40] Preeti Malakar, Prasanna Balaprakash, Venkatram Vishwanath, Vitali Morozov, and Kalyan Kumar. 2018. Benchmarking machine learning methods for performance modeling of scientific applications. In *2018 IEEE/ACM Performance Modeling, Benchmarking and Simulation of High Performance Computer Systems (PMBS)*. IEEE, 33–44.
- [41] Aniruddha Marathe, Rushil Anirudh, Nikhil Jain, Abhinav Bhatele, Jayaraman Thiagarajan, Bhavya Kailkhura, Jae-Seung Yeom, Barry Rountree, and Todd Gamblin. 2017. Performance modeling under resource constraints using deep transfer learning. In *Proceedings of the International Conference for High Performance Computing, Networking, Storage and Analysis*. 1–12.
- [42] Morteza Mardani, Gonzalo Mateos, and Georgios B Giannakis. 2015. Subspace learning and imputation for streaming big data matrices and tensors. *IEEE Transactions on Signal Processing* 63, 10 (2015), 2663–2677.
- [43] Charith Mendis, Alex Renda, Saman Amarasinghe, and Michael Carbin. 2019. Ithemal: Accurate, portable and fast basic block throughput estimation using deep neural networks. In *International Conference on machine learning*. PMLR, 4505–4515.
- [44] Harshitha Menon, Abhinav Bhatele, and Todd Gamblin. 2020. Auto-tuning parameter choices in HPC applications using bayesian optimization. In *2020 IEEE International Parallel and Distributed Processing Symposium (IPDPS)*. IEEE, 831–840.
- [45] Steven Karl Morley, Thiago Vasconcelos Brito, and Daniel T Wellings. 2018. Measures of model performance based on the log accuracy ratio. *Space Weather* 16, 1 (2018), 69–88.
- [46] Philipp Neumann. 2019. Sparse grid regression for performance prediction using high-dimensional run time data. In *European Conference on Parallel Processing*. Springer, 601–612.
- [47] Emin Nuriyev and Alexey Lastovetsky. 2021. Efficient and Accurate Selection of Optimal Collective Communication Algorithms Using Analytical Performance Modeling. *IEEE Access* 9 (2021), 109355–109373.
- [48] Fabian Pedregosa, Gaël Varoquaux, Alexandre Gramfort, Vincent Michel, Bertrand Thirion, Olivier Grisel, Mathieu Blondel, Peter Prettenhofer, Ron Weiss, Vincent Dubourg, et al. 2011. Scikit-learn: Machine learning in Python. *the Journal of machine Learning research* 12 (2011), 2825–2830.
- [49] Fabrizio Petrini, Darren J Kerbyson, and Scott Pakin. 2003. The case of the missing supercomputer performance: Achieving optimal performance on the 8,192 processors of ASCI Q. In *SC'03: Proceedings of the 2003 ACM/IEEE conference on Supercomputing*. IEEE, 55–55.
- [50] Dirk Pflüger. 2010. *Spatially Adaptive Sparse Grids for High-Dimensional Problems*. Verlag Dr. Hut, München. <http://www5.in.tum.de/pub/pflueger10spatialy.pdf>
- [51] Dirk Pflüger. 2012. Spatially Adaptive Refinement. In *Sparse Grids and Applications (Lecture Notes in Computational Science and Engineering)*, Jochen Garske and Michael Griebel (Eds.). Springer, Berlin Heidelberg, 243–262. http://www5.in.tum.de/pub/pflueger12spatialy_preprint.pdf
- [52] Thomas Rauber and G Rünger. 2000. Modelling the runtime of scientific programs on parallel computers. In *Proceedings 2000. International Workshop on Parallel Processing*. IEEE, 307–314.
- [53] David F Richards, Omar Aziz, Jeanine Cook, Hal Finkel, Brian Homerding, Tanner Judeman, Peter McCorquodale, Tiffany Mintz, and Shirley Moore. 2018. *Quantitative performance assessment of proxy apps and parents*. Technical Report. Lawrence Livermore National Lab.(LLNL), Livermore, CA (United States)
- [54] Rohan Basu Roy, Tirthak Patel, Vijay Gadepally, and Devesh Tiwari. 2021. Bliss: auto-tuning complex applications using a pool of diverse lightweight learning models. In *Proceedings of the 42nd ACM SIGPLAN International Conference on Programming Language Design and Implementation*. 1280–1295.
- [55] Kijung Shin and U Kang. 2014. Distributed methods for high-dimensional and large-scale tensor factorization. In *2014 IEEE International Conference on Data Mining*. IEEE, 989–994.
- [56] Navjot Singh, Zecheng Zhang, Xiaoxiao Wu, Naijing Zhang, Siyuan Zhang, and Edgar Solomonik. 2022. Distributed-memory tensor completion for generalized loss functions in Python using new sparse tensor kernels. *J. Parallel and Distrib.*

- Comput.* 169 (2022), 269–285.
- [57] Shaden Smith, Jongsoo Park, and George Karypis. 2016. An exploration of optimization algorithms for high performance tensor completion. In *SC'16: Proceedings of the International Conference for High Performance Computing, Networking, Storage and Analysis*. IEEE, 359–371.
- [58] Sergei Abramovich Smolyak. 1963. Quadrature and interpolation formulas for tensor products of certain classes of functions. In *Doklady Akademii Nauk*, Vol. 148. Russian Academy of Sciences, 1042–1045.
- [59] Edgar Solomonik, Devin Matthews, Jeff R Hammond, John F Stanton, and James Demmel. 2014. A massively parallel tensor contraction framework for coupled-cluster computations. *J. Parallel and Distrib. Comput.* 74, 12 (2014), 3176–3190.
- [60] Qingquan Song, Xiao Huang, Hancheng Ge, James Caverlee, and Xia Hu. 2017. Multi-aspect streaming tensor completion. In *Proceedings of the 23rd ACM SIGKDD international conference on knowledge discovery and data mining*. 435–443.
- [61] Dan Stanzione, Bill Barth, Niall Gaffney, Kelly Gaither, Chris Hempel, Tommy Minyard, S. Mehringer, Eric Werner, H. Tufo, D. Panda, and P. Teller. 2017. Stampede 2: The Evolution of an XSEDE Supercomputer. In *Proceedings of the Practice and Experience in Advanced Research Computing 2017 on Sustainability, Success and Impact* (New Orleans, LA, USA) (PEARC17). ACM, New York, NY, USA, Article 15, 8 pages. <https://doi.org/10.1145/3093338.3093385>
- [62] Benoit Steiner, Chris Cummins, Horace He, and Hugh Leather. 2021. Value learning for throughput optimization of deep learning workloads. *Proceedings of Machine Learning and Systems* 3 (2021), 323–334.
- [63] Ondřej Sýkora, Phitchaya Mangpo Phothilimthana, Charith Mendis, and Amir Yazdanbakhsh. 2022. GRANITE: A Graph Neural Network Model for Basic Block Throughput Estimation. In *2022 IEEE International Symposium on Workload Characterization (IISWC)*. IEEE, 14–26.
- [64] Nathan R Tallent and Adolfy Hoisie. 2014. Palm: Easing the burden of analytical performance modeling. In *Proceedings of the 28th ACM international conference on Supercomputing*. 221–230.
- [65] Philippe Tillet and David Cox. 2017. Input-aware auto-tuning of compute-bound HPC kernels. In *Proceedings of the International Conference for High Performance Computing, Networking, Storage and Analysis*. 1–12.
- [66] Chris Tofallis. 2015. A better measure of relative prediction accuracy for model selection and model estimation. *Journal of the Operational Research Society* 66, 8 (2015), 1352–1362.
- [67] Giorgio Tomasi and Rasmus Bro. 2005. PARAFAC and missing values. *Chemometrics and Intelligent Laboratory Systems* 75, 2 (2005), 163–180.
- [68] Richard Vuduc, James W Demmel, and Jeff A Bilmes. 2004. Statistical models for empirical search-based performance tuning. *The International Journal of High Performance Computing Applications* 18, 1 (2004), 65–94.
- [69] Stephen Wright, Jorge Nocedal, et al. 1999. Numerical optimization. *Springer Science* 35, 67–68 (1999), 7.
- [70] Xingfu Wu, Prasanna Balaprakash, Michael Kruse, Jaehoon Koo, Brice Videau, Paul Hovland, Valerie Taylor, Brad Geltz, Siddhartha Jana, and Mary Hall. 2023. ytpt: Autotuning Scientific Applications for Energy Efficiency at Large Scales. *arXiv preprint arXiv:2303.16245* (2023).
- [71] Xingfu Wu, Michael Kruse, Prasanna Balaprakash, Hal Finkel, Paul Hovland, Valerie Taylor, and Mary Hall. 2022. Autotuning PolyBench benchmarks with LLVM Clang/Polly loop optimization pragmas using Bayesian optimization. *Currency and Computation: Practice and Experience* 34, 20 (2022), e6683.
- [72] Rio Yokota. 2013. An FMM based on dual tree traversal for many-core architectures. *Journal of Algorithms & Computational Technology* 7, 3 (2013), 301–324.
- [73] Harry Yserentant. 1992. Hierarchical bases. In *Proceedings of the second international conference on Industrial and applied mathematics*. 256–276.

Appendix: Artifact Description/Artifact Evaluation

ARTIFACT IDENTIFICATION

We propose and evaluate low rank tensor decomposition for modeling application performance. We discretize the input and configuration domain of an application using regular grids. Application execution times mapped within grid-cells are averaged and represented by tensor elements. We show that low-rank canonical-polyadic (CP) tensor decomposition is effective in approximating these tensors. We further show that this decomposition enables accurate extrapolation of unobserved regions of an application’s parameter space. We then employ tensor completion to optimize a CP decomposition given a sparse set of observed runtimes. We consider alternative piecewise/grid-based models and supervised learning models for six applications and demonstrate that CP decomposition optimized using tensor completion offers higher prediction accuracy and memory-efficiency for high-dimensional applications.

We present a software library for this proposed performance model that leverages open-source high-performance software for tensor completion and which may be found at <https://github.com/huttered40/cpr-perf-model>. We describe our benchmarking methodology in . Here, we provide some more technical details to allow reproduction of our results on the Blue Waters machine All experimental results were performed using this public repository and may be reproduced using the exact scripts that it provides.

REPRODUCIBILITY OF EXPERIMENTS

The experimental workflow to use our performance model consists of two main steps. The first step (1) consists of dataset generation to facilitate training and testing the model. All benchmark parameters and corresponding benchmark runtime must be specified in these datasets. The final step (2) consists of training and testing the model using these datasets, which is done by launching the corresponding program. We provide the datasets for all six benchmarks specified in the paper here: https://github.com/huttered40/app_ed.

Step (2) consists of executing more than 100 scripts and executing more than 1000 Python programs. We estimate that full reproducibility of the experimental results listed in the paper, starting from step (2), takes about 10-20 hours. This time accounts for up to 9 distinct performance modeling methods, up to 6 different benchmarks, up to 10 distinct training set sizes, and as many as 100 distinct hyper-parameter settings for each method. We provide the complete list of scripts necessary to reproduce the experimental results listed in our paper in the public Github repository: <https://github.com/huttered40/cpr-perf-model>. Specifically, the subdirectory at <https://github.com/huttered40/cpr-perf-model/tree/main/reproducibility> stores all of the scripts necessary to reproduce every figure in the paper. Execution of each script generates a corresponding CSV file that must then be parsed (e.g., via gnuplot) to reproduce the figure.

In the reproducibility README, we provide the exact versions of each Python library we used. This information alone should suffice to reproduce our experimental results irrespective of the machine it

is executed on. We refer to the Experimental Methodology section of the paper for specific details describing how each script is run. The expected results from the experiment workflow are equivalent to those found in the article, as we followed the same workflow when generating results.